Carbon 139 (2018) 581–585

Contents lists available at ScienceDirect

Carbon

journal homepage: www.elsevier.com/locate/carbon

Raman resonance profile of an individual confined long linear carbon chain

Sebastian Heeg [a, *], Lei Shi [b], Thomas Pichler [b], Lukas Novotny [a]

[a] ETH Zürich, Photonics Laboratory, 8093 Zürich, Switzerland
[b] University of Vienna, Faculty of Physics, 1090 Wien, Austria

ARTICLE INFO

Article history:
Received 22 May 2018
Received in revised form
26 June 2018
Accepted 4 July 2018
Available online 6 July 2018

ABSTRACT

This paper reports tip-enhanced, polarization dependent and excitation energy dependent Raman measurements of an individual long linear carbon chain confined in a double-walled carbon nanotube. We determine the band gap of the chain (2.093 eV) from a Raman resonance profile with a line width $\Gamma = 145$ meV, which corresponds to a lifetime of $\tau = 4.5$ fs for the excited state of the chain. In the absence of external perturbations, this suggests that the chain's excited state dynamics depend on the confinement inside the nanotube and therefore on the chirality of the encasing carbon nanotube.

1. Introduction

Long linear carbon chains (LLCCs) encapsulated inside carbon nanotubes are the finite realisation of carbyne, an infinitely long chain of carbon atoms forming the truly one-dimensional allotrope of carbon [1,2]. The tubes act as nano-reactors allowing for chain growth, protect the chains from the environment, and enable the formation of long linear carbon chains that may comprise of several thousands of atoms [3–7]. Due to a Peierls distortion, the confined chains are polyynic with alternating single and triple bonds. This bond-length alteration (BLA) results in the formation a band gap E_G of up to several eV and is the origin of the only Raman active vibration of the chain (C-mode), a longitudinal-optical phonon corresponding to the in-phase stretching of the triple bonds [8,9].

Raman spectroscopy is a powerful tool to characterise confined chains as the C-mode directly reports the chain's BLA and the Raman characteristics of the encasing carbon nanotubes are well known. It has enabled the study of pressure, charge transfer, and screening effects on the chains and their nanotubes hosts, and revealed that the chirality of the encasing nanotube determines the BLA and hence the band gap and the C-mode frequency of the encapsulated LLCC [6,10–12]. The importance of Raman spectroscopy in characterising confined LLCCs is highlighted by the fact that the carbon nanotube hosts prohibit alternative direct optical methods such as absorption or photoluminescence spectroscopy by spectral overlap or quenching, respectively [13].

Resonant Raman enhancement of the chain's C-mode occurs if the excitation energy E_L is close to or coincides with the bandgap E_G of the corresponding chain [14]. Mapping the C-mode's Raman intensity as a function of E_L is called Raman resonance profile (RRP) or resonance window. The RRP reveals the exact energy of the band gap. The width Γ of the RRP carries information on the dynamics of the chain's excited electronic state, because it is related to the state's lifetime τ by $\Gamma = \hbar/\tau$ [14]. *Shi* et al. measured Raman resonance profiles of six C-mode frequency bands (1793–1856 cm^{-1}) from bulk quantities of LLCCs encapsulated in double-walled carbon nanotubes (DWCNTs) [5]. They determined the corresponding band gaps (1.848–2.253 eV), and confirmed that the well known linear relation with the C-mode frequency also holds for long linear carbon chains. The width Γ of the RRPs, however, varied from 72 meV to 145 meV. It remained unclear whether the observed Γ – values are intrinsic to the corresponding chains or inhomogeneously broadened. The latter occurs for LLCCs with very similar C-mode frequencies and band gaps that cannot be separated in bulk Raman measurements.

Here we report for the first time a Raman resonance profile of an individual, confined long linear carbon chain. The presence of a single chain is confirmed by tip-enhanced Raman scattering (TERS) and polarization dependent, confocal Raman measurements in resonance with the chain's band gap. Excitation energy dependent Raman measurements yield a resonance window $\Gamma = 145 \pm 10$ meV, which corresponds to an excited state lifetime of $\tau \sim 4.5$ fs. We find strong evidence that τ is intrinsic to the confined

* Corresponding author.
E-mail address: sheeg@ethz.ch (S. Heeg).
URL: https://www.photonics.ethz.ch

https://doi.org/10.1016/j.carbon.2018.07.007
0008-6223/

chain investigated here and suggest that the chirality of the encasing nanotubes defines the lifetime of the confined chain's excited electronic state.

2. Experimental

2.1. Sample preparation

The long linear carbon chains encapsulated inside double-walled carbon nanotubes, c.f. Fig. 1 (a), were obtained by annealing DWCNTs in form of buckypaper at 1460 °C for 1 h in vacuum (8.2×10^{-7} mbar) [3]. To prepare the individualised DWCNTs with the confined chains, the annealed buckypaper (~0.1 mg) was dissolved in benzenesulfonic acid (~1 mL). A droplet of the obtained solution was dropcasted onto a glass coverslip, where it remained for 15 min. Subsequently, the coverslip was immersed in chloroform for 10 min, baked at 115 °C for 20 min, immersed in diethyl ether for 5 min, baked again at 115 °C for another 20 min, rinsed by water, and finally dried by nitrogen gas. All purification and dispersion steps were performed in an oxygen-free environment.

2.2. Raman spectroscopy

TERS was performed in backscattering configuration using a home-built setup whose details are described elsewhere [6]. In short, a radially polarized laser beam ($E_L = 1.96$ eV) was focussed by an oil-immersion objective (NA 1.4) through a thin glass coverslip. Placing the apex of an Au pyramid in the laser focus, c.f. Fig. 1(b), creates an intense local excitation source, which enables the high spatial resolution and local Raman enhancement characteristic for TERS [15]. The Raman scattered light was collected by a combination of a bandpass – set to transmit the C-mode of LLCCs – and an avalanche photodetector for imaging or a combination of spectrograph and charge-coupled device of spectral acquisition.

Polarization and excitation energy dependent Raman measurements were performed with a spectrometer in single grating and backscattering configuration and an air objective (NA 0.9). By placing a polarizer before the spectrometer entrance slit, we probe only the Raman scattered light that is linearly polarized parallel to the excitation laser. To vary the polarization direction Θ we inserted a $\lambda/2$ – plate between the beam splitter of the focusing microscope and the microscope objective. This configuration, shown in Fig. 2(a), simultaneously rotates the polarization of the incoming, linearly polarized and the Raman scattered light and removes any polarization dependence in the detection path of the spectrometer. A dye laser (Rhodamine 6G) was used as tunable excitation source (2.03–2.20 eV) which we varied in steps of 5–15 meV. The wavelength dependent Raman measurements were calibrated and normalised using the Raman peak position and intensity of diamond, respectively.

Both Raman setups are equipped with XY-piezo-stages for scanning. On the TERS setup, integration times were 25 ms/pixel for imaging and 60 s for Raman spectra with laser powers of 150 μW measured before the back aperture of the objective. On the tunable excitation setup, integration times ranged between 10 s for mapping and up to 120 s for single spectra. The laser power was kept below 150 μW to avoid sample degradation.

3. Results and discussion

A confocal Raman spectrum of the long linear carbon chain investigated in this study is shown in Fig. 1(c) for $E_L = 1.96$ eV (633 nm) measured on the TERS setup. The peak at 1834 cm^{-1} is the chain's C-mode and the G-modes of the encasing nanotubes are found just below 1600 cm^{-1}. We observe no D-mode, indicating

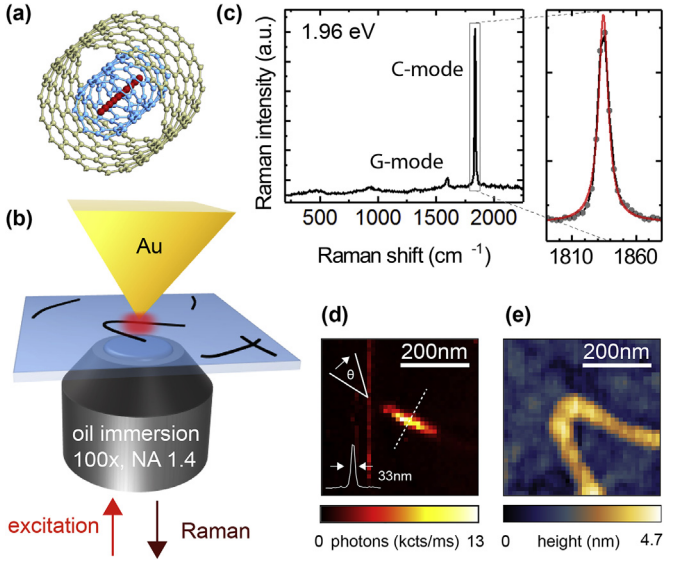

Fig. 1. Tip-enhanced Raman characterization of an individual linear carbon chain. (a) Long linear carbon chain (red) encapsulated in double-walled carbon nanotube (blue/yellow). (b) Schematic of our TERS setup. (c) Confocal Raman spectrum of linear carbon chain's C-mode at 1834 cm^{-1} and the CNT G-modes just below 1600 cm^{-1}. (d) TERS C-mode image of long linear carbon chain. (e) Topography acquired simultaneously with the image in (d). (A colour version of this figure can be viewed online.)

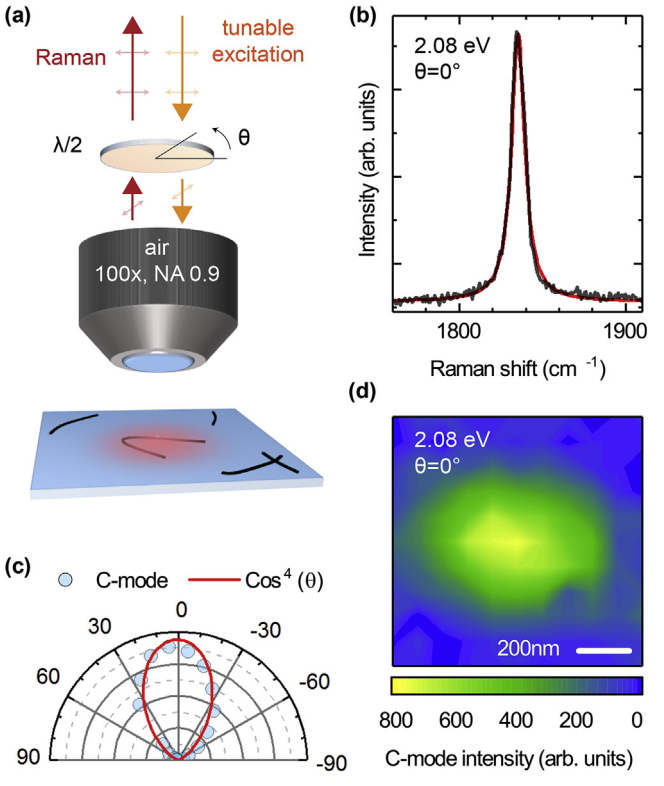

Fig. 2. Polarization dependent and spatially resolved resonant Raman scattering of an individual linear carbon chain excited at $E_L = 2.08$ eV. (a) Illustration of setup used for polarization- and wavelength dependent Raman measurements. (b) Resonant Raman spectrum of the isolated linear carbon chain shown in Fig. 1(c) with both the incoming and the scattered light polarized along the chain axis (Θ = 0°). (c) Polarization dependent Raman intensity of the chain's C-mode as a function of Θ at 2.08 eV. (d) Confocal Raman map of the chain's C-mode acquired with a stepsize of 100 nm. (A colour version of this figure can be viewed online.)

that the nanotubes are largely free of defects [16]. The C-mode is well described by a single Lorentzian fit, shown in the inset of Fig. 1(c), with a full width at half-maximum (FWHM) of 9.4 cm^{-1}, which is among the smallest values reported on single LLCCs [3,6,7]. Both the symmetric shape and FWHM of the C-mode provide strong evidence that the Raman signal arises from a single, isolated chain.

To confirm the isolated, single nature of the chain investigated here we placed the TERS tip near the sample surface and simultaneously recorded high resolution TERS and topography images, as shown in Fig. 1(d) and (e), respectively. The TERS image shows the continuous signature of a single encapsulated chain of length 180 nm. A line profile extracted from the TERS image, inset in Fig. 1(d), implies a resolution of 33 nm. The topography in Fig. 1(e) reveals that the DWCNT (average outer tube diameter ~1.3 nm) [3] containing the chain is part of a small bundle of ~3.5 nm in height. The presence of additional tubes does not affect our measurements as we are interested in the chain's Raman signatures only.

In the following we discuss the properties of the encapsulated chain when excited close to its optical band gap, which we expect at ~2.07 eV based on the linear relation between C-mode frequency and band gap established experimentally in Ref. [5]. Fig. 2(b) shows the C-mode of the chain excited at 2.08 eV (596 nm). A single Lorentzian fit describes the C-mode very well and yields a Raman shift of 1834 cm^{-1} and FWHM of 9.6 cm^{-1}. Both peak position and FWHM are in excellent agreement with the values obtained for 1.96 eV (633 nm), Fig. 1(b). This confirms that we observe the same chain as before and that no other chain contributes to the observed Raman response.

The Raman spectrum of the chain shown in Fig. 2(b) was measured with the polarization of the incident and Raman scattered light parallel to the orientation of the chain ($\Theta = 0°$), where Θ is the angle between the chain and the polarization direction, c.f. Fig. 1(d). Rotating the $\lambda/2$ – plate, c.f. Fig. 2(b), allows us to probe the polarization dependence of the chain's Raman response. The spectral position and the FWHM of the C-mode do not change as a function of Θ (not shown) and shift less than ± 0.8 cm^{-1} around the mean values, which we understand as the experimentally available precision.

However, we observe a strong change in the integrated C-mode scattering intensities $I(\Theta)$ shown in Fig. 2(c), which is excellently described by $I(\Theta) \sim \cos^4\Theta$ and plotted (red) in Fig. 2(c). This functional form occurs for a Raman tensor where all elements R_{ij} vanish except for R_{zz} with z parallel to the CNT/chain axis. The Raman scattering intensity arises only from the projection of the incoming and scattered light onto the chain axis. This dependence is well known for one-dimensional systems like carbon nanotubes or J-aggregated molecules and originates from a depolarisation or antenna effect [16–18]. It is also expected for the fully symmetric $A_{1g}(\Sigma_g^+)$ Raman active C-mode of the chain, and confirmed here experimentally for the first time.[1] All Raman measurements discussed in the following are taken with $\Theta = 0°$.

A confocal Raman map of the chain's integrated C-mode intensity for $E_L = 2.08$ eV is shown in Fig. 2(d). It reproduces very well the location, spatial extent and orientation of the chain, c.f. Fig. 1(d) and (e). The highest C-mode intensity is measured when the laser focus is centered on the chain. To ensure that we record the maximum intensity for all excitation energy dependent measurements discussed in the following, we acquired Raman maps as shown in Fig. 2(d) for each E_L before taking single spectra with extended integration times at the location of the highest C-mode intensity.

The excitation energy dependent, normalised Raman spectra of the chain are presented in Fig. 3(a). For all excitation energies, a strong C-mode dominates the spectrum. The G-modes of the nanotubes appear as comparably weak features just below 1600 cm^{-1}. Lorentzian fits reveal that both the spectral position and the FWHM for all C-mode peaks shown in Fig. 3(a) are independent of E_L and remain constant to within ≤ 1 cm^{-1}.

In Fig. 3(b), we present the integrated Raman intensity of the chain (dots) as a function of excitation energy. A clear intensity maximum, corresponding to an electronic resonance of the chain, is observed. In analogy to the analysis of the bulk measurements in Ref. [5], we fit the resonance Raman profile using a semiclassical resonance Raman model

$$I(E_L) = \left| \frac{M}{E_L - E_G - i\frac{\Gamma}{2}} \right|^2, \quad (1)$$

and obtain $E_G = 2.093 \pm 0.00$ eV for the optical band gap of the chain and $\Gamma = 145 \pm 9$ meV for the width of the Raman resonance profile. M describes all coupling matrix elements and serves as a free parameter for the fit. Eq. (1) describes our experimental data very well and is plotted as the brown line in Fig. 3(b).

Equation (1) only considers the case where the incident light is in resonance (incoming resonance) with E_G and neglects resonances of the scattered light (outgoing resonance) at higher excitation energies. As for the bulk measurements in Ref. [5], this is justified because the energetic separation between the incoming and outgoing resonances is large (~225 meV), and the range of

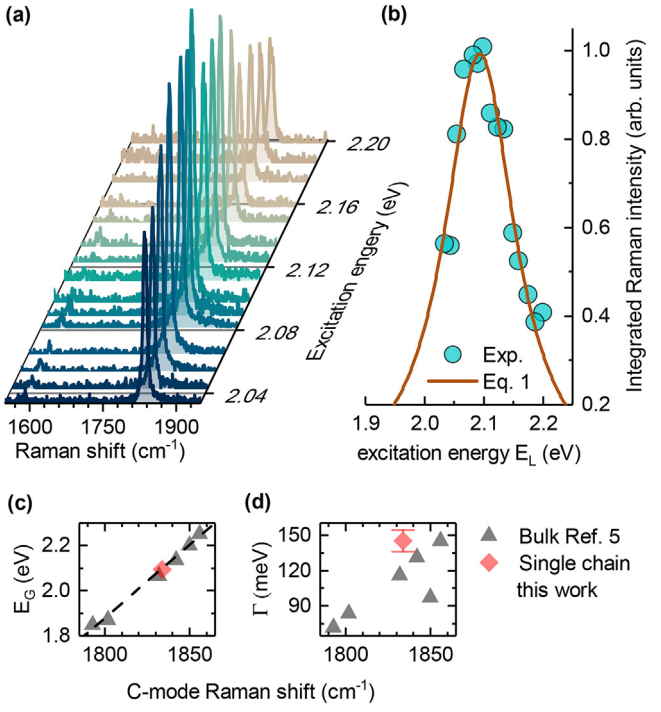

Fig. 3. Raman resonance profile of an individual long linear carbon chain. (a) Raman spectra of the chain recorded at different excitation energies. The spectra are coloured and offset for clarity. (b) Raman resonance profile of the chain extracted from the spectra in (a). The intensities are normalised to the maximum intensity. (c) Band gap E_G and resonance width Γ as a function of C-mode frequency observed for bulk measurements (triangles, Ref. [5]) and the single chain measured in this work (diamond) are shown in (c) and (d), respectively. (A colour version of this figure can be viewed online.)

[1] A polyynic linear carbon chain belongs to the $D_{\infty h}$ point group. Sometimes the symmetry of the chain's C-mode is falsely given as Σ^+ instead of Σ_g^+ in the literature.

excitation energies available for our experiment covers only the incoming resonance. At the same time, however, this prevents us from exploring the exact nature of optical transitions in linear carbon chains, as measuring the outgoing resonances can in principle determine whether the optical transition of chains are band-to-band transitions, excitons, or must be described within the framework of Raman scattering of molecules [19–22]. Importantly, this uncertainty does not affect the conclusions of this work. In accordance with literature, we therefore use the term band gap to describe optical transitions in linear carbon chains.

The band gap E_G of the chain measured in this work is in excellent agreement with the linear correlation between C-mode and E_G observed for bulk measurements, c.f. Fig. 3(c). This confirms that we have indeed determined this chain's fundamental bandgap. Note that for single chain measurements it is common to observe C-modes that differ from bulk values, as the latter is dominated by the most abundant C-mode frequencies [6].

The width Γ of the chain's RRP shown in Fig. 3(d) is larger than what is those reported in Ref. [5] for chains with similar C-mode frequencies. To verify that Γ is intrinsic to the chain investigated here and that it can be faithfully compared to bulk values, we discuss in the following mechanisms that may reduce the lifetime of the chain's excited electronic states – and broaden Γ – such as environmental or temperature effects.

The lifetime of excited electronic states in carbon nanotubes can be strongly affected by their surrounding via charge transfer or dielectric screening, i.e. by the choice of surfactant in aqueous solutions or bundling effects [23–25]. The interior of a nanotube, however, is a highly unperturbed environment which effectively protects encapsulated objects like fullerenes, dye molecules or an additional inner nanotube from external influences [18,26–29]. This shielding effect is even more pronounced inside double-walled carbon nanotubes, where two concentric walls protect the confined LLCCs.

The interaction with a substrate may radially deform a nanotube, which breaks the symmetry of the chain-nanotube hybrid system and affects the lifetime τ of the chain's excited state [21]. For single-walled carbon nanotubes, these deformations occur for diameters > 2nm, and will take place for even larger diameter in the case of DWCNTs encasing the chain. However, LLCCs only form in DWCNTs with outer nanotube diameters below 1.75 nm [3]. Together with the high pressure stability of DWCNTs demonstrated in Ref. [30], we conclude that the chains are not affected by the environment outside the nanotubes both for bulk (DWCNTs in large bundle/bucky paper) and single chain measurements (small DWCNT bundles on glass), and that external effects yield no line broadening.

Bulk Raman measurements on LLCCs encapsulated in DWCNTs showed that the C-mode intensity increases fivefold and its FWHM decreases from 13 cm^{-1} to 6 cm^{-1} upon decreasing the temperature from 325 K to 38 K [3]. Laser induced heating of the chain investigated here should therefore result in a decreased C-mode intensity, an increased FWHM, and possibly a spectral shift of the C-mode.[2] For our excitation energy dependent measurements the laser intensities varied by a factor of up to 2.3. No trend of the C-mode position ($1833.9 \pm 1\ cm^{-1}$) or FWHM ($9.7 \pm 1\ cm^{-1}$) with increased laser intensities emerged, suggesting the absence of laser-induced heating. Our polarization-dependent measurements, c.f. Fig. 2, support this finding, considering that rotating the laser polarization effectively scales the chain's light absorption $\sim \cos^2\Theta$, which is equivalent to varying the laser intensity by more than an order of magnitude.

[2] The temperature dependent C-mode shift of confined linear carbon chains has not been determined experimentally.

It follows that $\Gamma = 145$ meV and the corresponding lifetime of the excited electronic state $\tau = 4.5$ fs is intrinsic to the encapsulated chain investigated here. This has two important consequences. First, the variation of Γ for chains with different C-mode frequencies observed in bulk measurements, c.f. Fig. 3(d), is a true feature, even though some of the bulk values may still be subject to inhomogeneous broadening. Second, Γ does not correlate with the C-mode frequency/band gap, and is therefore not directly dependent on the bond-length alteration of the chain. This may seem surprising at first, because the electronic, phononic and (predicted) mechanical properties of LLCCs change continuously with the BLA.

We can understand the variation of Γ qualitatively considering that the local environment experienced by the confined LLCC changes with the chirality of the encasing nanotube. We argue that the nanotube host affects the relaxation dynamics of the chain's excited electronic state and that this interaction depends on the nanotube's electronic structure that varies with chirality. A possible mechanism is Förster resonant energy transfer (FRET), where energy is transferred from a donor (chain) to an acceptor (nanotube) by non-radiative dipole-dipole coupling [31]. The efficiency of FRET scales with the distance between donor and acceptor, the relative orientation of their dipole moments, and the spectral overlap of the respective emission and absorption spectra. While the small distance between the nanotube and the encapsulated chain, and the parallel alignment of their dipole moments suggests an efficient energy transfer, these parameters do not depend of the nanotube's chirality. The optical transitions of the encasing nanotubes, however, vary strongly with chirality [16]. It is therefore the chirality of the encasing nanotube that determines the spectral overlap with chain's band gap, which modulates the efficiency of the energy transfer and determines the lifetime on the chain's excited electronic state.

Experimentally, the absence of luminescence emission from the encapsulated chains speaks in favour of efficient energy transfer. It must be mentioned, however, that to the best of our knowledge the dependence of the chain's lifetime on the host nanotube chirality has not been studied theoretically. The importance of chirality has been highlighted in a recent theoretical study on the optical response of carbon chains inside single-walled carbon nanotubes [32]. Furthermore, it was shown that the chirality of the encasing nanotubes uniquely determines the electronic (band gap) and phononic (C-mode) properties of confined linear carbon chains [6]. Combining this with our findings suggests that double-walled nanotubes of the same chirality contain LLCCs with the same C-mode frequency, the same bandgap, and the same excited state lifetime. While the C-mode and the bandgap of the chain scale approximately linearly with the inner nanotube diameter, Γ varies as a function of chirality. This explains why long linear carbon chains with very similar C-mode frequencies, c.f. Fig. 3(d), differ in Γ.

4. Conclusions

In conclusion, we have measured the length, the polarization dependence and the Raman resonance profile of a single, isolated long linear carbon chain encapsulated inside a double-walled carbon nanotube. We find that the width of the resonance profile is intrinsic to the investigated chain, suggesting that the carbon nanotube chirality determines the excited state dynamics of the encapsulated long linear carbon chain.

Acknowledgments

The authors acknowledge W. Wenseleers and S. Cambre for fruitful discussions. We thank L. V. Poulikakos for fabricating the Au

pyramids and S. Reich for access to the Raman system allowing for tunable excitation wavelength measurements. This research was supported by the Swiss National Science Foundation (grant no. 200021-165841) and the Austrian Science Funds (FWF, P27769-N20). S. Heeg acknowledges financial support by ETH Zurich Career Seed Grant SEED-16 17-1.

References

[1] C.S. Casari, M. Tommasini, R.R. Tykwinski, A. Milani, Carbon-atom wires: 1-D systems with tunable properties, Nanoscale 8 (8) (2016) 4414–4435, https://doi.org/10.1039/c5nr06175j.
[2] C. Casari, A. Milani, Carbyne: from the elusive allotrope to stable carbon atom wires, MRS Commun. (2018) 1Ð13, https://doi.org/10.1557/mrc.2018.48.
[3] L. Shi, P. Rohringer, K. Suenaga, Y. Niimi, J. Kotakoski, J.C. Meyer, H. Peterlik, M. Wanko, S. Cahangirov, A. Rubio, Z.J. Lapin, L. Novotny, P. Ayala, T. Pichler, Confined linear carbon chains as a route to bulk carbyne, Nat. Mater. 15 (6) (2016) 634–639, https://doi.org/10.1038/nmat4617.
[4] M. Wanko, S. Cahangirov, L. Shi, P. Rohringer, Z.J. Lapin, L. Novotny, P. Ayala, T. Pichler, A. Rubio, Polyyne electronic and vibrational properties under environmental interactions, Phys. Rev. B 94 (19) (2016), 195422, https://doi.org/10.1103/PhysRevB.94.195422.
[5] L. Shi, P. Rohringer, M. Wanko, A. Rubio, S. Wasserroth, S. Reich, S. Cambre, W. Wenseleers, P. Ayala, T. Pichler, Electronic band gaps of confined linear carbon chains ranging from polyyne to carbyne, Phys. Rev. Mater. 1 (7) (2017) 075601–075607, https://doi.org/10.1103/PhysRevMaterials.1.075601.
[6] S. Heeg, L. Shi, L. V. Poulikakos, T. Pichler, and L. Novotny, Carbon nanotube chirality determines properties of encapsulated linear carbon chain, arXiv 1711.04753v2.
[7] Z.J. Lapin, R. Beams, L.G. Cançado, L. Novotny, Near-field Raman spectroscopy of nanocarbon materials, Faraday Discuss 184 (2015) 193–206, https://doi.org/10.1039/C5FD00050E.
[8] J. Kastner, H. Kuzmany, L. Kavan, F.P. Dousek, J. Kürti, Reductive preparation of carbyne with high-yield - an in-situ Raman-Scattering study, Macromolecules 28 (1) (1995) 344–353, https://doi.org/10.1021/ma00105a048.
[9] J. Kürti, H. Kuzmany, Resonance Raman-Scattering from finite and infinite polymer-chains, Phys. Rev. B 44 (2) (1991) 597–613, https://doi.org/10.1103/PhysRevB.44.597.
[10] L.G. Moura, L.M. Malard, M.A. Carneiro, P. Venezuela, R.B. Capaz, D. Nishide, Y. Achiba, H. Shinohara, M.A. Pimenta, Charge transfer and screening effects in polyynes encapsulated inside single-wall carbon nanotubes, Phys. Rev. B 80 (16) (2009) 161401–161404, https://doi.org/10.1103/PhysRevB.80.161401.
[11] N.F. Andrade, A.L. Aguiar, Y.A. Kim, M. Endo, P.T.C. Freire, G. Brunetto, D.S. Galvão, M.S. Dresselhaus, A.G. Souza Filho, Linear carbon chains under high-pressure conditions, J. Phys. Chem. C 119 (19) (2015) 10669–10676, https://doi.org/10.1021/acs.jpcc.5b00902.
[12] W.Q. Neves, R.S. Alencar, R.S. Ferreira, A.C. Torres-Dias, N.F. Andrade, A. San-Miguel, Y.A. Kim, M. Endo, D.W. Kim, H. Muramatsu, A.L. Aguiar, A.G.S. Filho, Effects of pressure on the structural and electronic properties of linear carbon chains encapsulated in double wall carbon nanotubes, Carbon 133 (2018) 446–456, https://doi.org/10.1016/j.carbon.2018.01.084.
[13] P. Rohringer, L. Shi, P. Ayala, T. Pichler, Selective enhancement of inner tube photoluminescence in filled double-walled carbon nanotubes, Adv. Funct. Mater. 26 (27) (2016) 4874–4881, https://doi.org/10.1002/adfm.201505502.
[14] P. Yu, M. Cardona, Fundamentals of Semiconductors, Physics and Materials Properties, Springer Science & Business Media, Berlin, Heidelberg, 2010, https://doi.org/10.1007/978-3-642-00710-1.
[15] T.W. Johnson, Z.J. Lapin, R. Beams, N.C. Lindquist, S.G. Rodrigo, L. Novotny, S.-H. Oh, Highly reproducible near-field optical imaging with sub-20-nm resolution based on template-stripped gold pyramids, ACS Nano 6 (10) (2012) 9168–9174, https://doi.org/10.1021/nn303496g.
[16] S. Reich, C. Thomsen, J. Maultzsch, Carbon Nanotubes: an Introduction to the Basic Concepts and Physical Properties, Wiley-VCH New York, 2004.
[17] G.S. Duesberg, I. Loa, M. Burghard, K. Syassen, S. Roth, Polarized Raman spectroscopy on isolated single-wall carbon nanotubes, Phys. Rev. Lett. 85 (25) (2000) 5436–5439, https://doi.org/10.1103/PhysRevLett.85.5436.
[18] N.S. Mueller, S. Heeg, P. Kusch, E. Gaufrès, N.Y.W. Tang, U. Hübner, R. Martel, A. Vijayaraghavan, S. Reich, Plasmonic enhancement of SERS measured on molecules in carbon nanotubes, Faraday Discuss 00 (2017) 1–19, https://doi.org/10.1039/C7FD00127D.
[19] C. Thomsen, S. Reich, Raman Scattering in Carbon Nanotubes, in Light Scattering in Solid IX, Springer, Berlin, Heidelberg, 2006, pp. 115–234, https://doi.org/10.1007/978-3-540-34436-03.
[20] H.N. Tran, J.C. Blancon, J.-R. Huntzinger, R. Arenal, V.N. Popov, A.A. Zahab, A. Ayari, A. San-Miguel, F. Vallée, N. Del Fatti, J.L. Sauvajol, M. Paillet, Excitonic optical transitions characterized by Raman excitation profiles in single-walled carbon nanotubes, Phys. Rev. B 94 (7) (2016) 075430–075436, https://doi.org/10.1103/PhysRevB.94.075430.
[21] J.-C. Blancon, M. Paillet, H.-N. Tran, X.-T. Than, S.A. Guebrou, A. Ayari, A.S. Miguel, N.-M. Phan, A.-A. Zahab, J.-L. Sauvajol, F.V.e. e, N. Del Fatti, Direct measurement of the absolute absorption spectrum of individual semiconducting single-wall carbon nanotubes, Nat. Commun. 4 (2013) 1–8, https://doi.org/10.1038/ncomms3542.
[22] A.C. Albrecht, On the theory of Raman intensities, J. Chem. Phys. 34 (5) (1961) 1476–1484, https://doi.org/10.1063/1.1701032.
[23] J. Maultzsch, H. Telg, S. Reich, C. Thomsen, Radial breathing mode of single-walled carbon nanotubes: optical transition energies and chiral-index assignment, Phys. Rev. B 72 (20) (2005), 205438, https://doi.org/10.1103/PhysRevB.72.205438.
[24] S. Reich, M. Dworzak, A. Hoffmann, C. Thomsen, M.S. Strano, Excited-state Carrier lifetime in single-walled carbon nanotubes, Phys. Rev. B 71 (3) (2005), 033402, https://doi.org/10.1103/PhysRevB.71.033402.
[25] J.S. Park, Y. Oyama, R. Saito, W. Izumida, J. Jiang, K. Sato, C. Fantini, A. Jorio, G. Dresselhaus, M.S. Dresselhaus, Raman resonance window of single-wall carbon nanotubes, Phys. Rev. B 74 (16) (2006), https://doi.org/10.1103/PhysRevB.74.165414, 286–6.
[26] L. Kavan, L. Dunsch, H. Kataura, A. Oshiyama, M. Otani, S. Okada, Electrochemical tuning of electronic Structure of C 60 and C 70 Fullerene Peapods:~ in situ visible near-infrared and Raman study, J. Phys. Chem. B 107 (31) (2003) 7666–7675, https://doi.org/10.1021/jp035332f.
[27] M. Kalbac, L. Kavan, S. Gorantla, T. Gemming, L. Dunsch, Sexithiophene encapsulated in a single-walled carbon nanotube: an in situ Raman spectroelectrochemical study of a peapod structure, Chem. Eur J. 16 (38) (2010) 11753–11759, https://doi.org/10.1002/chem.201001417.
[28] E. Gaufrès, N.Y.W. Tang, F. Lapointe, J. Cabana, M.A. Nadon, N. Cottenye, F. Raymond, T. Szkopek, R. Martel, Giant Raman scattering from J-aggregated dyes inside carbon nanotubes for multispectral imaging, Nat. Photon. 8 (1) (2013) 72–78, https://doi.org/10.1038/nphoton.2013.309.
[29] R. Pfeiffer, H. Kuzmany, C. Kramberger, C. Schaman, T. Pichler, H. Kataura, Y. Achiba, J. Kürti, V. Zólyomi, Unusual high degree of unperturbed environment in the interior of single-wall carbon nanotubes, Phys. Rev. Lett. 90 (22) (2003) 162–164, https://doi.org/10.1103/PhysRevLett.90.225501.
[30] R.S. Alencar, W. Cui, A.C. Torres-Dias, T.F.T. Cerqueira, S. Botti, M.A.L. Marques, O.P. Ferreira, C. Laurent, A. Weibel, D. Machon, D.J. Dunstan, A.G.S. Filho, A. San-Miguel, Pressure-induced radial collapse in few-wall carbon nanotubes: a combined theoretical and experimental study, Carbon 125 (2017) 429–436, https://doi.org/10.1016/j.carbon.2017.09.044.
[31] L. Novotny, B. Hecht, Principles of Nano-optics, Cambridge University Press, 2012.
[32] F. Bonabi, S.J. Brun, T.G. Pedersen, Excitonic optical response of carbon chains confined in single-walled carbon nanotubes, Phys. Rev. B 96 (15) (2017), https://doi.org/10.1103/PhysRevB.96.155419, 155419–8.